

Accelerated and Adaptive Meshfree Methods

J. S. Chen, S. Yoon, Y. You, H. Lu, T. Xiao
University of California, Los Angeles

T. Voth
Sandia National Laboratories

C. T. Wu
Livermore Software Technology Corporation

H. P. Wang
General Motors R&D

**Sandia is a multiprogram laboratory operated by Sandia Corporation for the United States Department of Energy under contract DE-AC04-94AL850000*



OUTLINE

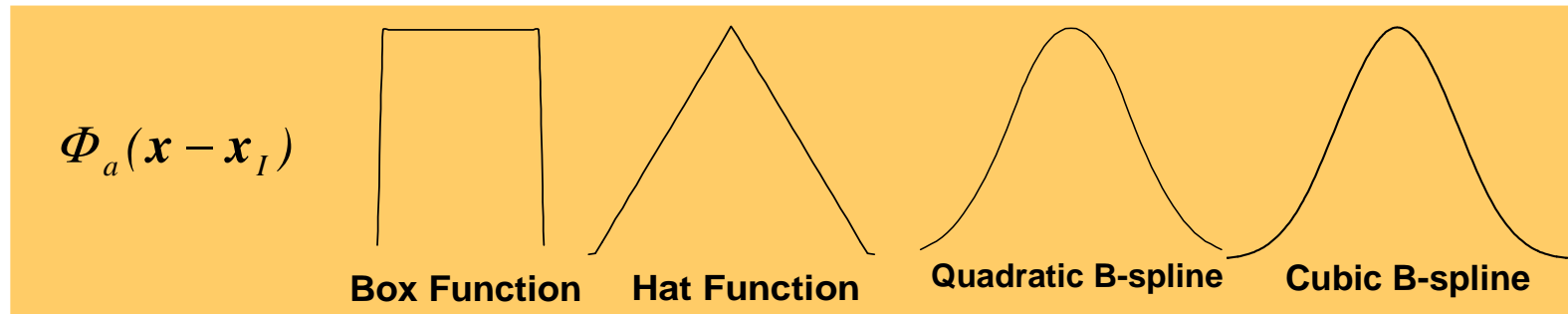
Robust meshfree formulation for large deformation and contact problems with application to simulation of metal forming processes

- Meshfree Formulation for Large Deformation Analysis
- Three Dimensional Meshfree Contact Formulation
- Enhanced Boundary Condition Treatments
- Stabilized Galerkin Meshfree Method
- Progressive Adaptivity Method
- Meshfree Simulation of Metal Forming Processes
- Other Applications



Discrete Reproducing Kernel Approximation

$$u^h(\mathbf{x}) = \sum_{I=1}^{NP} C(\mathbf{x}; \mathbf{x} - \mathbf{x}_I) \Phi_a(\mathbf{x} - \mathbf{x}_I) d_I$$



$$C(\mathbf{x}; \mathbf{x} - \mathbf{x}_I) = \sum_{i+j+k=0}^n (x_1 - x_{1I})^i (x_2 - x_{2I})^j (x_3 - x_{3I})^k b_{ijk}(\mathbf{x})$$

$$\sum_{I=1}^{NP} \Psi_I(\mathbf{x}) x_{1I}^i x_{2I}^j x_{3I}^k = x_1^i x_2^j x_3^k, \quad i + j + k = 0, \dots, n$$

$$\Rightarrow C(\mathbf{x}; \mathbf{x} - \mathbf{x}_I) = \mathbf{H}^T(\mathbf{0}) \mathbf{M}^{-1}(\mathbf{x}) \mathbf{H}(\mathbf{x} - \mathbf{x}_I)$$

$$\mathbf{M}(\mathbf{x}) = \sum_{I=1}^{NP} \mathbf{H}(\mathbf{x} - \mathbf{x}_I) \mathbf{H}^T(\mathbf{x} - \mathbf{x}_I) \Phi_a(\mathbf{x} - \mathbf{x}_I)$$

$$\mathbf{H}^T(\mathbf{x} - \mathbf{x}_I) = [1, x_1 - x_{1I}, \dots, (x_3 - x_{3I})^n]$$



Meshfree Formulation for Large Deformation Analysis

Lagrangian
weak form

$$\int_{\Omega_x} \delta u_{i,j} \tau_{ij} d\Omega_x = \int_{\Omega_X} \frac{\partial u_i}{\partial X_k} F_{kj}^{-1} \tau_{ij} J^0 d\Omega_X = \int_{\Omega_X} \frac{\partial u_i}{\partial X_k} \sigma_{ki} d\Omega_X$$

$$\int_{\Omega_x} \delta u_{i,j} (D_{ijkl} + T_{ijkl}) \Delta u_{k,l} d\Omega_x = \int_{\Omega_X} \frac{\partial \delta u_i}{\partial X_m} F_{mj}^{-1} (D_{ijkl} + T_{ijkl}) F_{nl}^{-1} \frac{\partial \Delta u_k}{\partial X_n} J^0 d\Omega_X$$

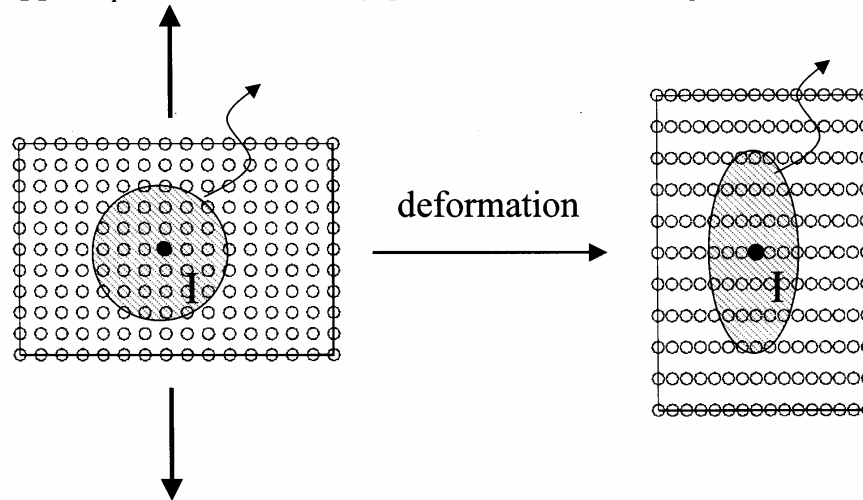
Lagrangian kernel
and shape function

$$\Psi_I^X(\mathbf{X}) = \mathbf{H}^T(\mathbf{0}) \mathbf{M}^{-1}(\mathbf{X}) \mathbf{H}(\mathbf{X} - \mathbf{X}_I) \Phi_a^X(\mathbf{X} - \mathbf{X}_I)$$

$$\frac{\partial \Psi_I^X(\mathbf{X})}{\partial x_i} = \frac{\partial \Psi_I^X(\mathbf{X})}{\partial X_j} \frac{\partial X_j}{\partial x_i} = \frac{\partial \Psi_I^X(\mathbf{X})}{\partial X_j} F_{ji}^{-1}$$

$$\mathbf{F}^{-1} = \left[\sum_{I=1}^{NP} \mathbf{d}_I \otimes \frac{\partial \Psi_I^X(\mathbf{X})}{\partial \mathbf{X}} + \mathbf{I} \right]^{-1}$$

$\text{supp}(\Psi_I^X)$ at initial configuration $\text{supp}(\Psi_I^X)$ at current configuration



Enhanced Boundary Condition Treatments

Meshfree shape functions do not possess Kronecker delta properties

Transformation
Method

$$\hat{d}_{iJ} = u_i^h(\mathbf{x}_J) = \sum_{I=1}^{NP} \Psi_I(\mathbf{x}_J) d_{iI} = \sum_{I=1}^{NP} L_{IJ} d_{iI}$$

$$d_{iI} = \sum_{K=1}^{NP} L_{IK}^{-T} \hat{d}_{iK}, \quad L_{IJ} = \Psi_I(\mathbf{x}_J)$$

$$u_i^h(\mathbf{x}) = \sum_{I=1}^{NP} \Psi_I(\mathbf{x}) d_{iI} = \sum_{I=1}^{NP} \sum_{K=1}^{NP} \Psi_I(\mathbf{x}) L_{IK}^{-T} \hat{d}_{iK} \equiv \sum_{K=1}^{NP} \hat{\Psi}_K(\mathbf{x}) \hat{d}_{iK}$$

Boundary Singular
Kernel Method

$$\tilde{\Psi}_I(\mathbf{x}) = C(\mathbf{x}; \mathbf{x} - \tilde{\mathbf{x}}_I) \frac{\Phi_a(\mathbf{x} - \tilde{\mathbf{x}}_I)}{\left[\left(\frac{x_1 - \tilde{x}_{1I}}{a_1} \right)^2 + \left(\frac{x_2 - \tilde{x}_{2I}}{a_2} \right)^2 + \left(\frac{x_3 - \tilde{x}_{3I}}{a_3} \right)^2 \right]^p}$$

$$\tilde{\Psi}_I(\tilde{\mathbf{x}}_I) = 1$$

$$\Rightarrow \tilde{\Psi}_I(\tilde{\mathbf{x}}_J) = 0 \Rightarrow u^h(\tilde{\mathbf{x}}_I) = u_I$$

$$\Psi_I(\tilde{\mathbf{x}}_I) = 0$$

Generalized
Reproducing
Kernel
Approximation

$$u^h(\mathbf{x}) = \sum_I [\hat{\Psi}_I(\mathbf{x}) + \bar{\Psi}_I(\mathbf{x})] u_I$$

$\hat{\Psi}_I(\mathbf{x})$: primitive function

$$\hat{\Psi}_I(\mathbf{x}) = \frac{\hat{\Phi}_{\hat{a}_I}(\mathbf{x} - \mathbf{x}_I)}{\hat{\Phi}_{\hat{a}_I}(\mathbf{0})}, \quad \hat{a}_I \text{ s.t. } \mathbf{x}_J \notin \hat{\Phi}_{\hat{a}_I}(\mathbf{x} - \mathbf{x}_I), \forall J \neq I$$

$\bar{\Psi}_I(\mathbf{x})$: enrichment function

$$\bar{\Psi}_I(\mathbf{x}) = \mathbf{H}^T(\mathbf{x} - \mathbf{x}_I) \mathbf{a}(\mathbf{x}) \bar{\Phi}_{\bar{a}_I}(\mathbf{x} - \mathbf{x}_I)$$

$$\mathbf{H}^T(\mathbf{x} - \mathbf{x}_I) = \{ 1, x_1 - x_{1I}, x_2 - x_{2I}, x_3 - x_{3I}, (x_1 - x_{1I})^2, \dots, (x_3 - x_{3I})^n \}$$

Reproducing Conditions:

$$\sum_I [\hat{\Psi}_I(\mathbf{x}) + \bar{\Psi}_I(\mathbf{x})] x_{1I}^i x_{2I}^j x_{3I}^k = x_1^i x_2^j x_3^k \quad 0 \leq i + j + k \leq n$$

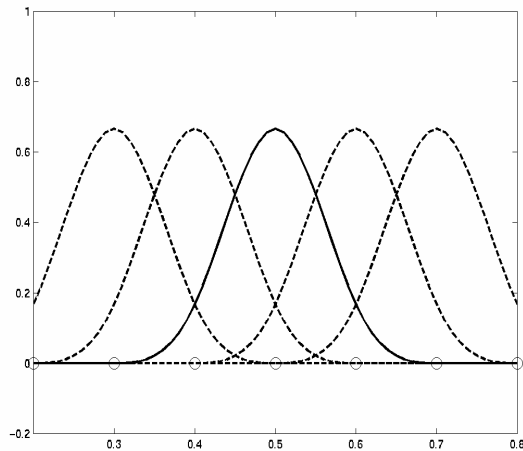
$$\Psi_I(\mathbf{x}) = \frac{\hat{\Phi}_{\hat{a}_I}(\mathbf{x} - \mathbf{x}_I)}{\hat{\Phi}_{\hat{a}_I}(\mathbf{0})} + \mathbf{H}^T(\mathbf{x} - \mathbf{x}_I) \mathbf{Q}^{-1}(\mathbf{x}) [\mathbf{H}(\mathbf{0}) - \hat{\mathbf{F}}(\mathbf{x})] \bar{\Phi}_{\bar{a}_I}(\mathbf{x} - \mathbf{x}_I)$$

$$\Rightarrow \Psi_I(\mathbf{x}_J) = \delta_{IJ}$$

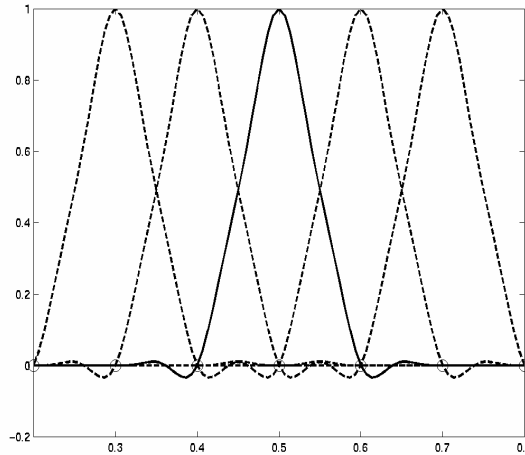
A Reproducing Kernel Interpolation

Properties of Reproducing Kernel Interpolation

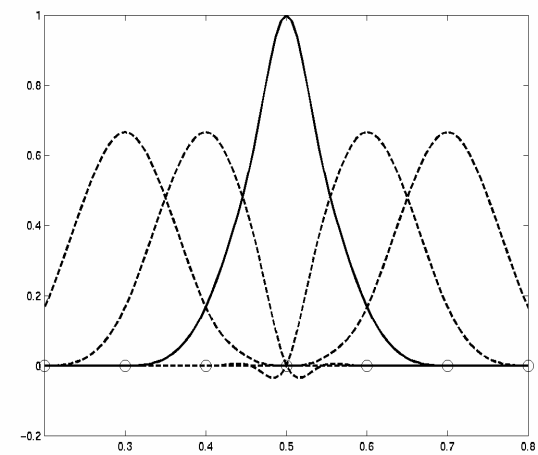
RK Approximation



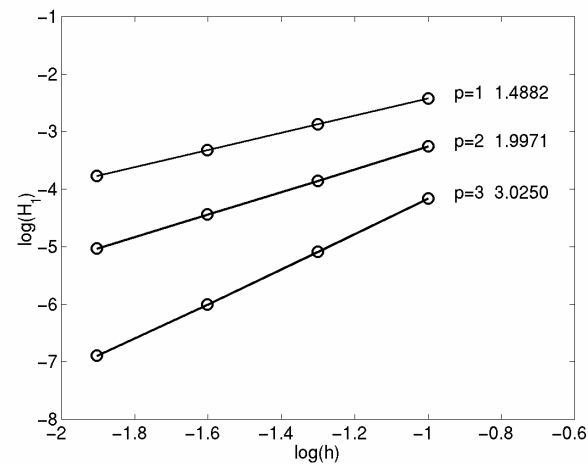
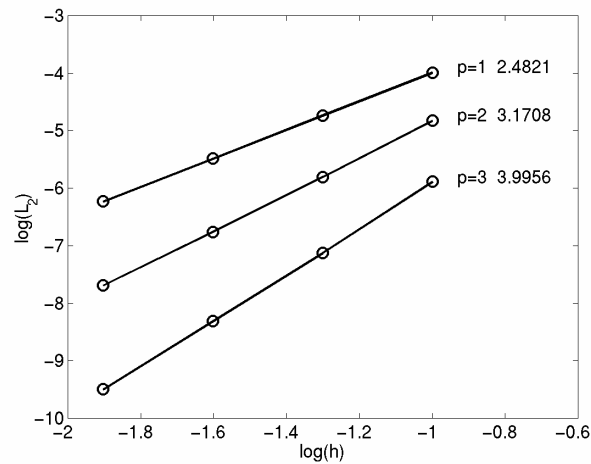
RK Interpolation



Mixed RK Interpolation



Convergence Rates $u_{,xx} = x^4$ in $(0,1)$, $u(0) = 0, u(1) = 0$



UCLA



Meshfree Contact Algorithm

Local approximation:

$$\mathbf{x}^R = f(x^*, y^*)$$

(x^*, y^*, z^*) : local coordinate

- $x^* - y^*$ projection plane
- Local least-square fit

At least C^2 continuity:

$$\mathbf{x}^R(x^*, y^*) = \sum_I \Psi_I^C(x^*, y^*) \mathbf{x}_I; \quad \Psi_I^C \in C^2$$

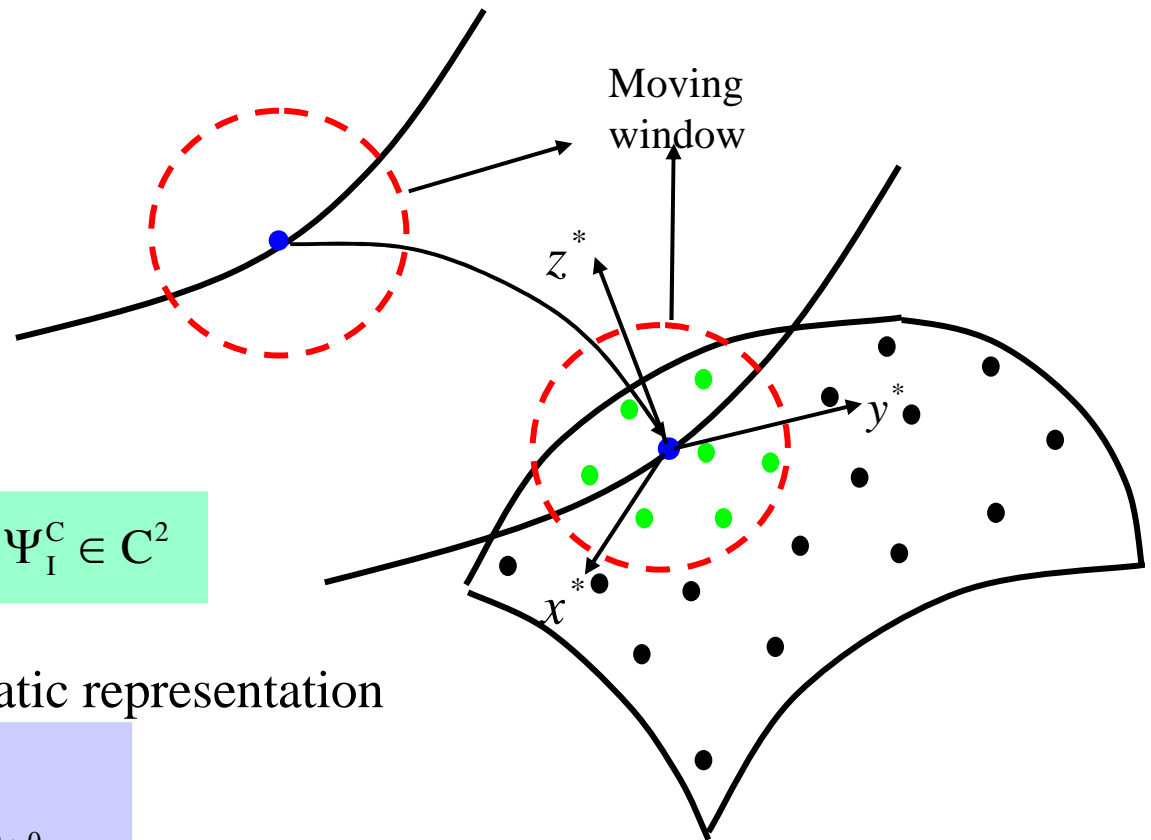
Consistent geometry and kinematic representation

$$(\mathbf{x}^R)^{v+1} = (\mathbf{x}^R)^0 + \Delta \mathbf{u}$$

$$(\mathbf{x}^R)^0(x^*, y^*) = \sum_I \Psi_I^C(x^*, y^*) (\mathbf{x}_I^R)^0$$

$$(\mathbf{x}^R)^{v+1}(x^*, y^*) = \sum_I \Psi_I^C(x^*, y^*) (\mathbf{x}_I^R)^{v+1}$$

$$\Delta \mathbf{u}(x^*, y^*) = \sum_I \Psi_I^C(x^*, y^*) \Delta \hat{\mathbf{d}}_I$$

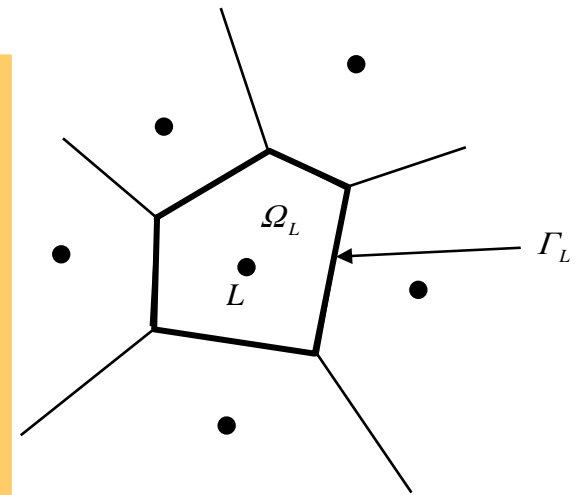


- Slave point
- Master point
- Local smooth surface control points

Accelerated Meshfree Method Based on a Stabilized Conforming Nodal Integration (SCNI)

Strain Smoothing

$$\begin{aligned}\bar{\varepsilon}_{ij}^h(\mathbf{x}_L) &= \frac{1}{2A_L} \int_{\Omega_L} (u_{i,j}^h + u_{j,i}^h) d\Omega \\ &= \frac{1}{2A_L} \int_{\Gamma_L} (u_i^h n_j + u_j^h n_i) d\Gamma = \frac{1}{2} [\bar{b}_{il}(\mathbf{x}_L) d_{jl} + \bar{b}_{jl}(\mathbf{x}_L) d_{il}] \\ \bar{b}_{il}(\mathbf{x}_L) &= \frac{1}{A_L} \int_{\Gamma_L} \Psi_I(\mathbf{x}) n_i d\Gamma \\ \sum_{L=1}^{NP} \bar{b}_{il}(\mathbf{x}_L) A_L &= \frac{1}{2} \sum_{L=1}^{NP} \int_{\Gamma_L} \Psi_I(\mathbf{x}) n_i d\Gamma = 0\end{aligned}$$



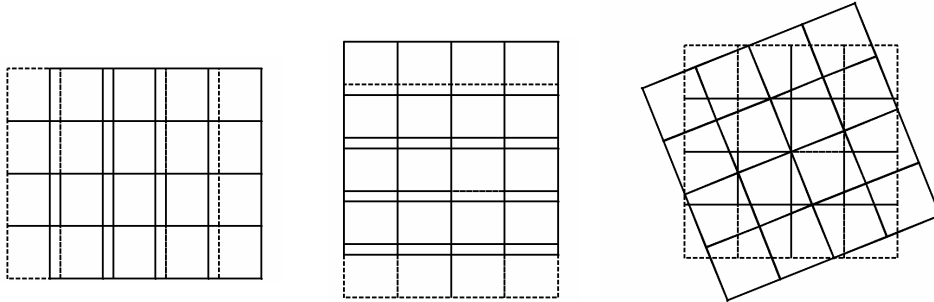
Stabilized Conforming Nodal Integration (SCNI)

$$\begin{aligned}\delta\Pi(\mathbf{u}, \bar{\varepsilon}) &= \int \delta\bar{\varepsilon}_{ij} C_{ijkl} \bar{\varepsilon}_{kl} d\Omega - \delta W^{ext}(\mathbf{u}) = 0 \\ \mathbf{u}^h(\mathbf{x}) &= \sum_{I=1}^{NP} \Psi_I(\mathbf{x}) \mathbf{d}_I, \quad \bar{\varepsilon}^h(\mathbf{x}) = \sum_{I=1}^{NP} \bar{\mathbf{B}}_I(\mathbf{x}) \mathbf{d}_I \\ \mathbf{K} \mathbf{d} &= \mathbf{f}, \quad \mathbf{K}_{IJ} = \sum_{L=1}^{NP} \bar{\mathbf{B}}_I^T(\mathbf{x}_L) \mathbf{C} \bar{\mathbf{B}}_J(\mathbf{x}_L) A_L\end{aligned}$$

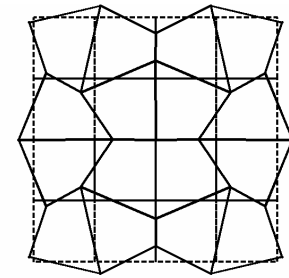
Eigenvalue Analysis

Direct Nodal Integration: 4 zero eigenvalues

3 zero eigenvalues: Rigid Body Modes

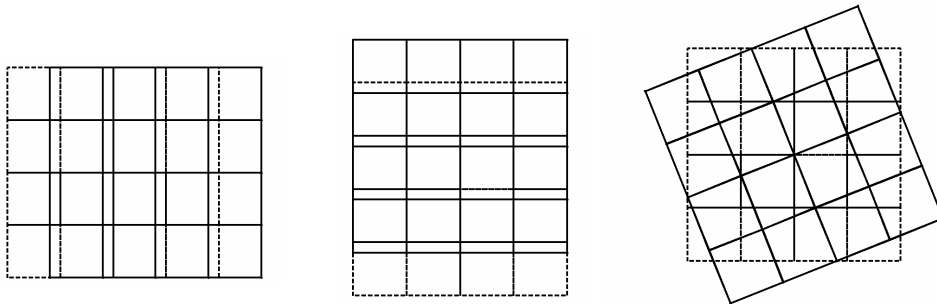


4th zero eigenvalue:
spurious zero energy mode

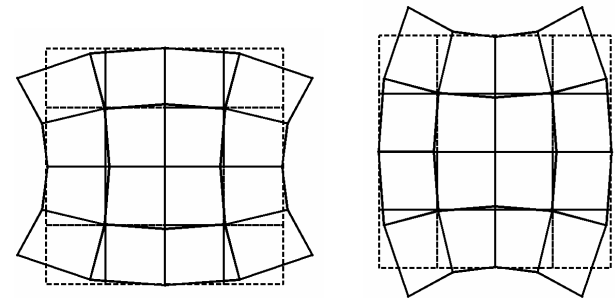


SCNI: 3 zero eigenvalues

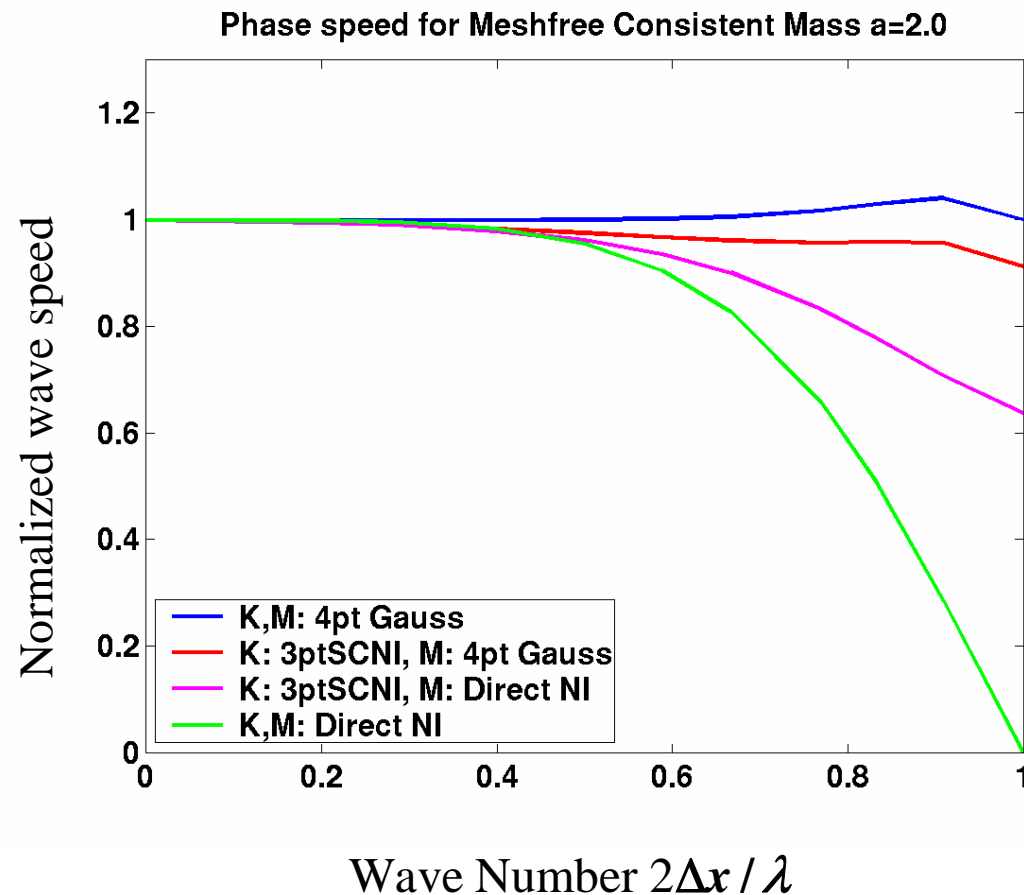
3 zero eigenvalues: Rigid Body Modes



4th smallest eigenvalue:
deformation modes

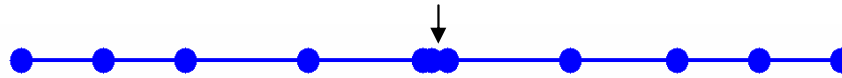


von Neumann Analysis of Dispersion Error Second Order Wave Equation

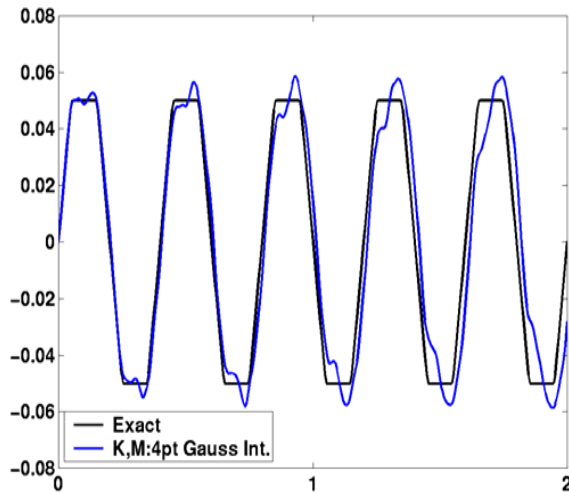


Transient Properties in Wave Problem

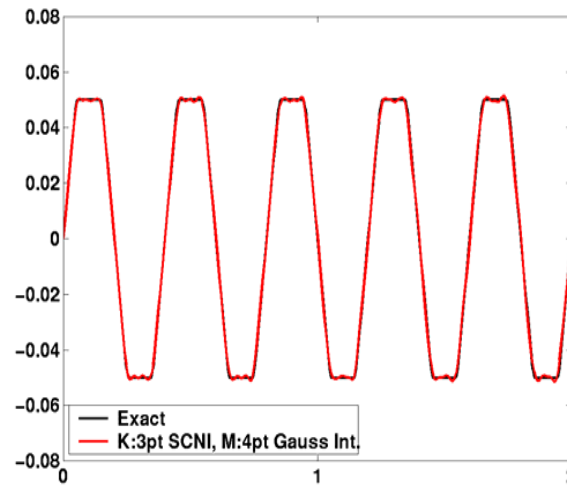
3pts almost overlapping



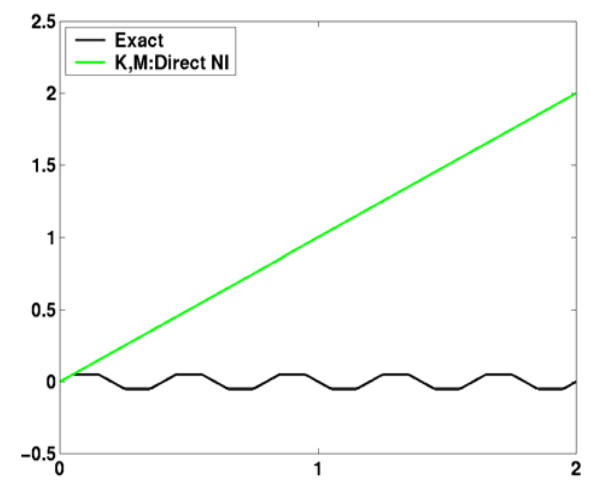
Gauss Integration



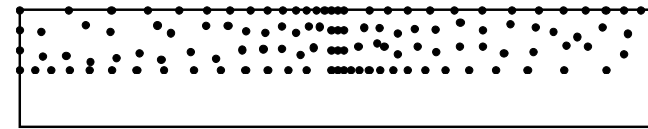
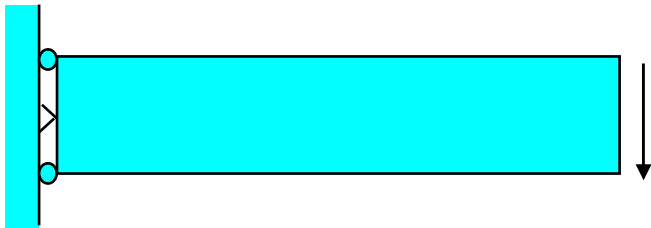
SC Nodal Integration



Direct Nodal Integration

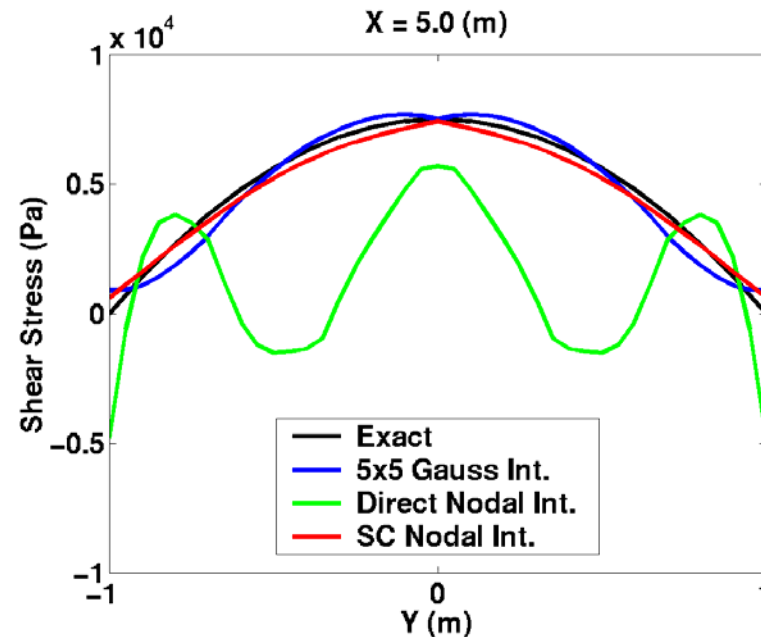
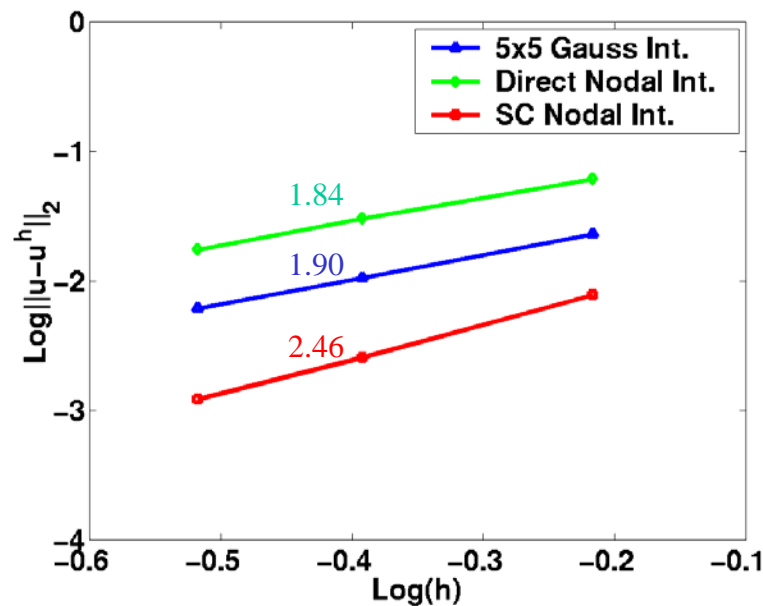


Convergence of Stabilized Conforming Nodal Integration



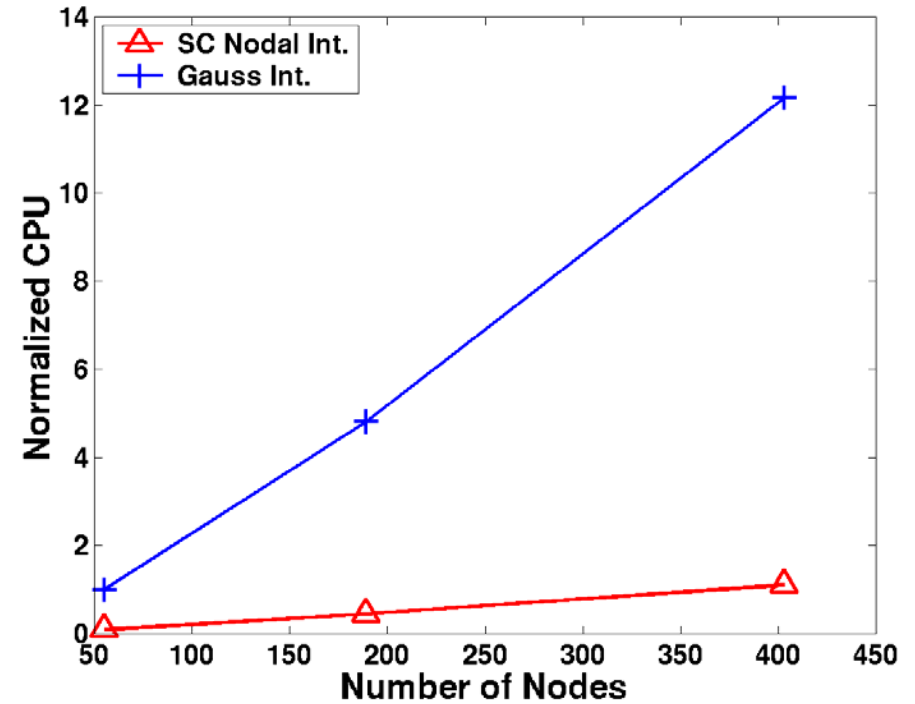
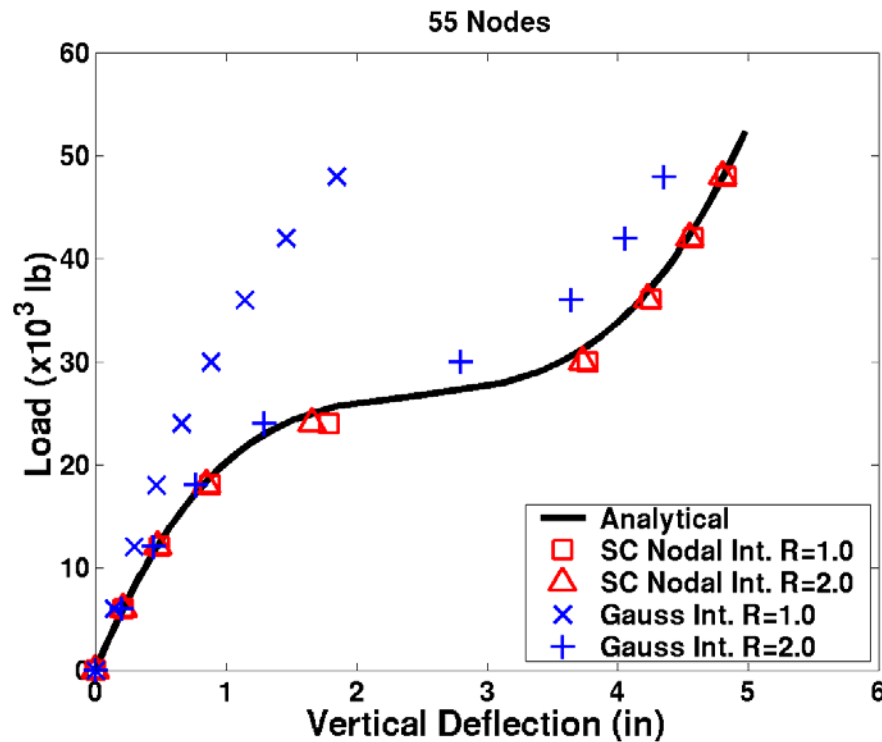
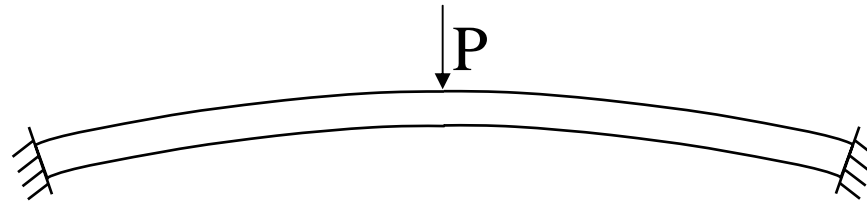
Tip displacement accuracy (%)

5x5 Gauss Int.	Direct Nodal Int.	SC Nodal Int.
94.99	192.82	99.25



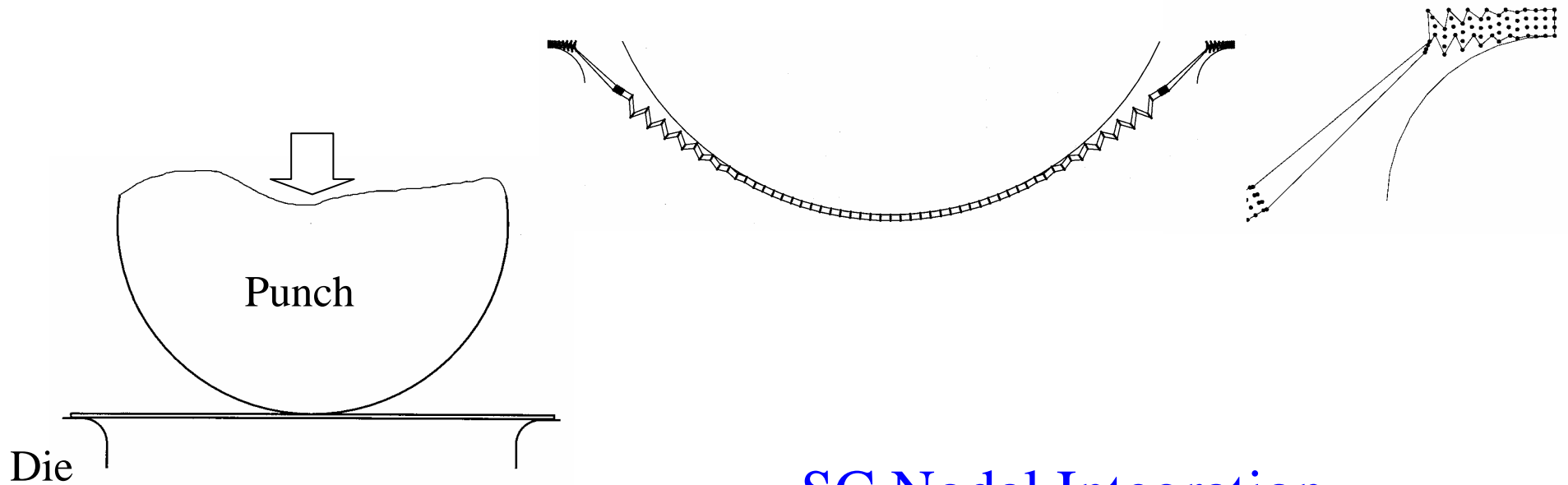
CPU ratio: 10~15:1

Shallow Arch Under a Point Load

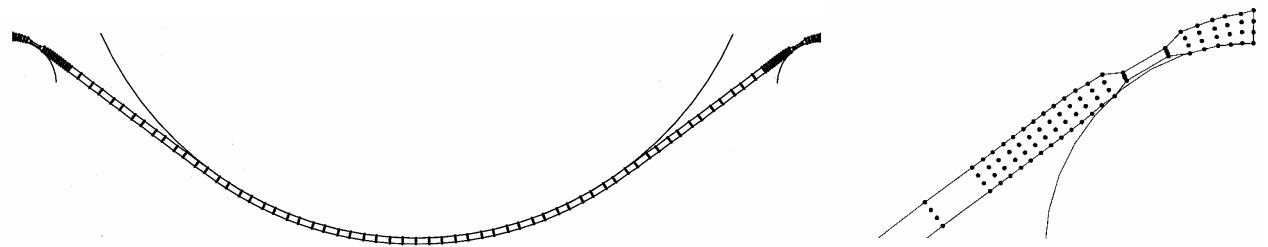


Cylindrical Punch

Direct Nodal Integration

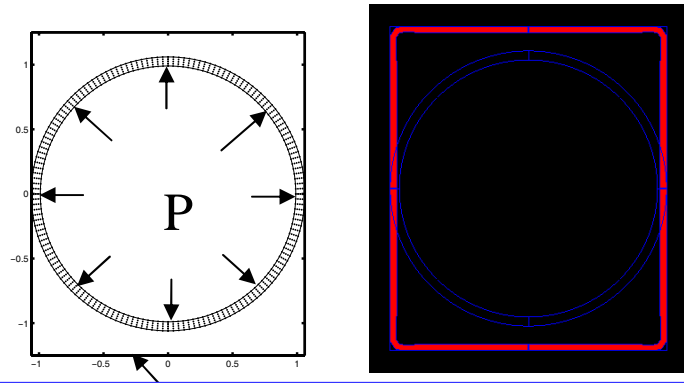


SC Nodal Integration

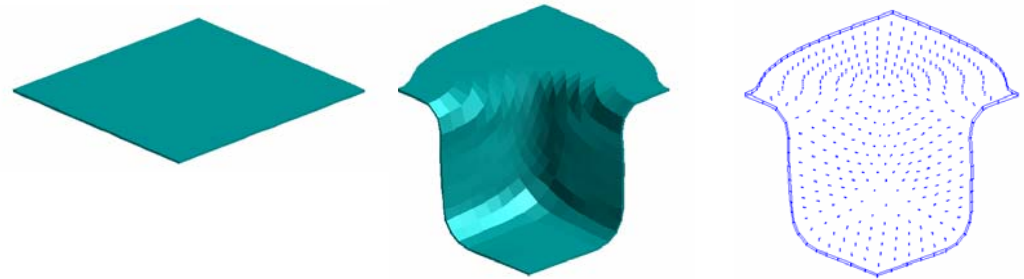


Metal Forming Simulation

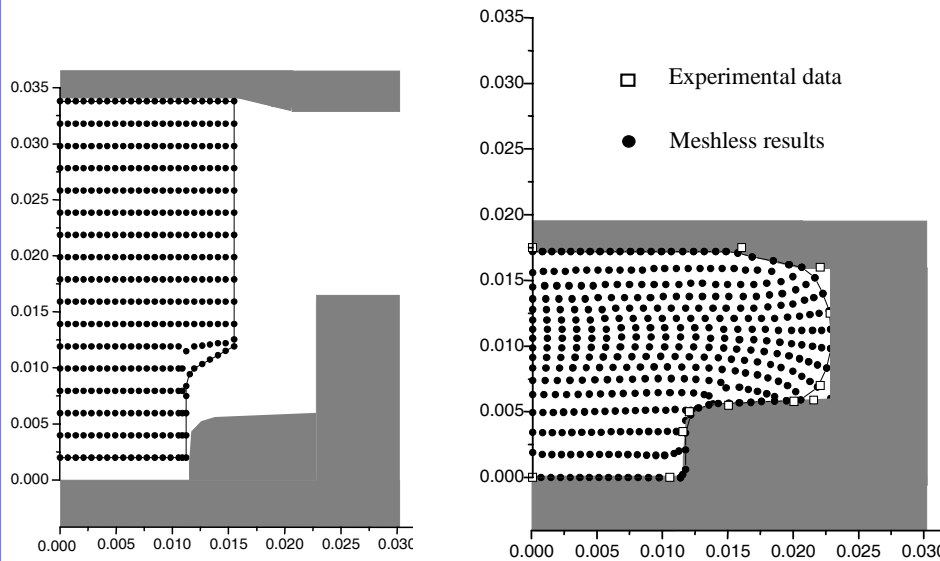
Hydroforming



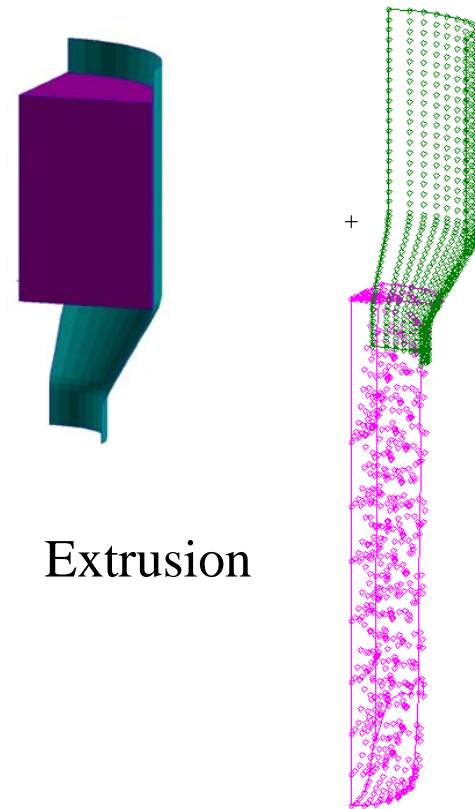
Deep Drawing



Forging



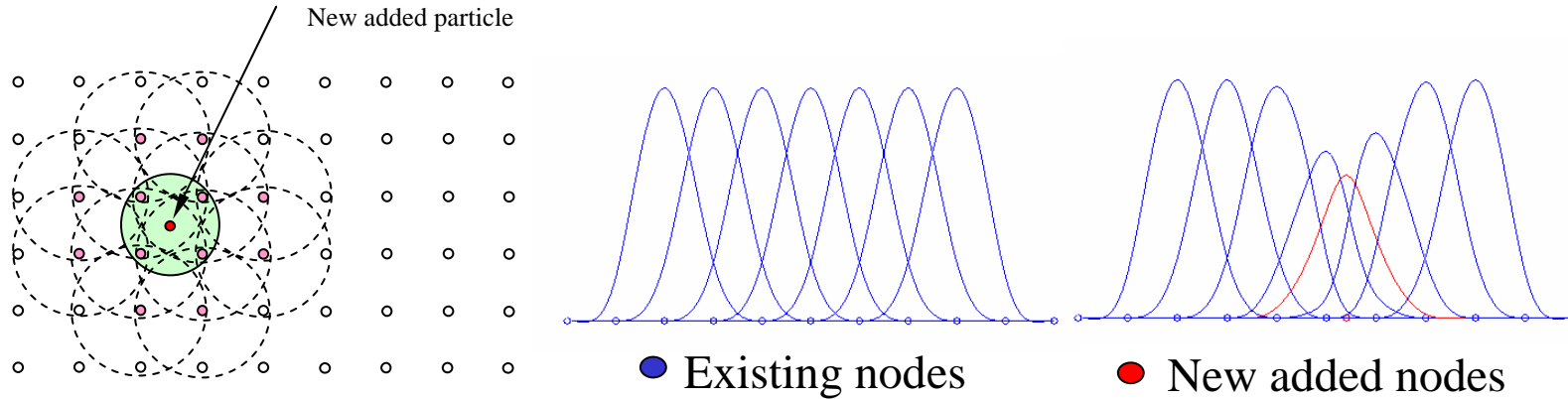
Extrusion



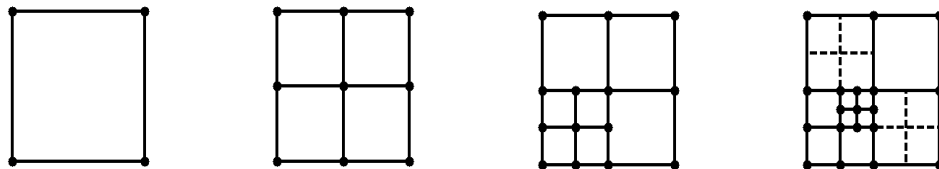
UCLA



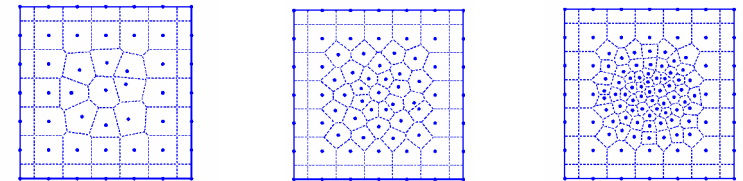
Adaptive Meshfree Method



Integration Cell Partitioning



Direct Node Insertion



$$\Psi_I(\mathbf{x}) = C(\mathbf{x}; \mathbf{x} - \mathbf{x}_I) \Phi_a(\mathbf{x} - \mathbf{x}_I) \quad C(\mathbf{x}; \mathbf{x} - \mathbf{x}_I) = \mathbf{H}^T(\mathbf{0}) \mathbf{M}^{-1}(\mathbf{x}) \mathbf{H}(\mathbf{x} - \mathbf{x}_I)$$

$$\mathbf{M}(\mathbf{x}) = \sum_{I=1}^{NP_{old}} \mathbf{H}(\mathbf{x} - \mathbf{x}_I) \mathbf{H}^T(\mathbf{x} - \mathbf{x}_I) \Phi_a(\mathbf{x} - \mathbf{x}_I) + \sum_{I=1}^{NP_{new}} \mathbf{H}(\mathbf{x} - \mathbf{x}_I) \mathbf{H}^T(\mathbf{x} - \mathbf{x}_I) \Phi_a(\mathbf{x} - \mathbf{x}_I)$$

$$= \mathbf{M}_{old}(\mathbf{x}) + \sum_{I=1}^{NP_{new}} \mathbf{H}(\mathbf{x} - \mathbf{x}_I) \mathbf{H}^T(\mathbf{x} - \mathbf{x}_I) \Phi_a(\mathbf{x} - \mathbf{x}_I)$$

Reproducing Kernel as a Low-Pass Filter

Reproducing kernel approximation

$$u^R(x) = u(x) * \Phi^a(x) = \int_{\Omega} u(\tilde{x}) \Phi^a(x - \tilde{x}) d\tilde{x}$$

$$u^R(x) = u(x) \hat{*} \Phi^a(x) = \sum_{I=1}^{NP} u(x_I) \Phi^a(x - x_I)$$

Reproducing properties

$$\sum_{I=1}^{NP} \Phi^a(x; x - x_I) x_I^k = x^k, \quad k = 0, 1, \dots, n$$

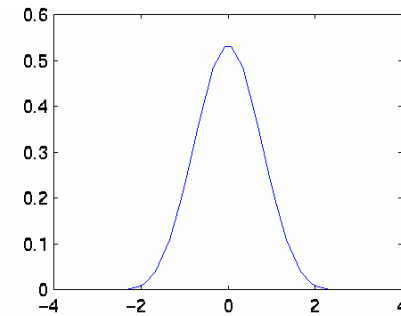
Low-pass filter properties

$$u(\tilde{x}) = \underbrace{u(x) + u'(x)(\tilde{x} - x) + \dots + \frac{1}{n!} u^{(n)}(x)(\tilde{x} - x)^n}_{u^L(\tilde{x})} + \underbrace{\frac{1}{(n+1)!} u^{(n+1)}(\xi)(\tilde{x} - x)^{n+1}}_{u^H(\tilde{x})}$$

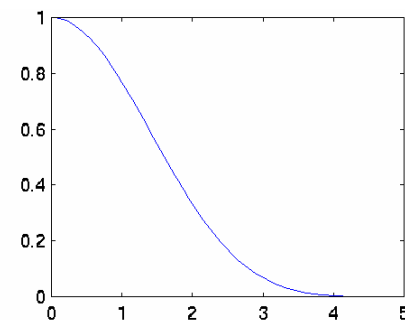
$$u^R(x) = u(x) \hat{*} \Phi^a(x) = [u^L(x) + u^H(x)] \hat{*} \Phi^a(x)$$

$$= u^L(x) + u^H(x) \hat{*} \Phi^a(x)$$

Reproducing Kernel



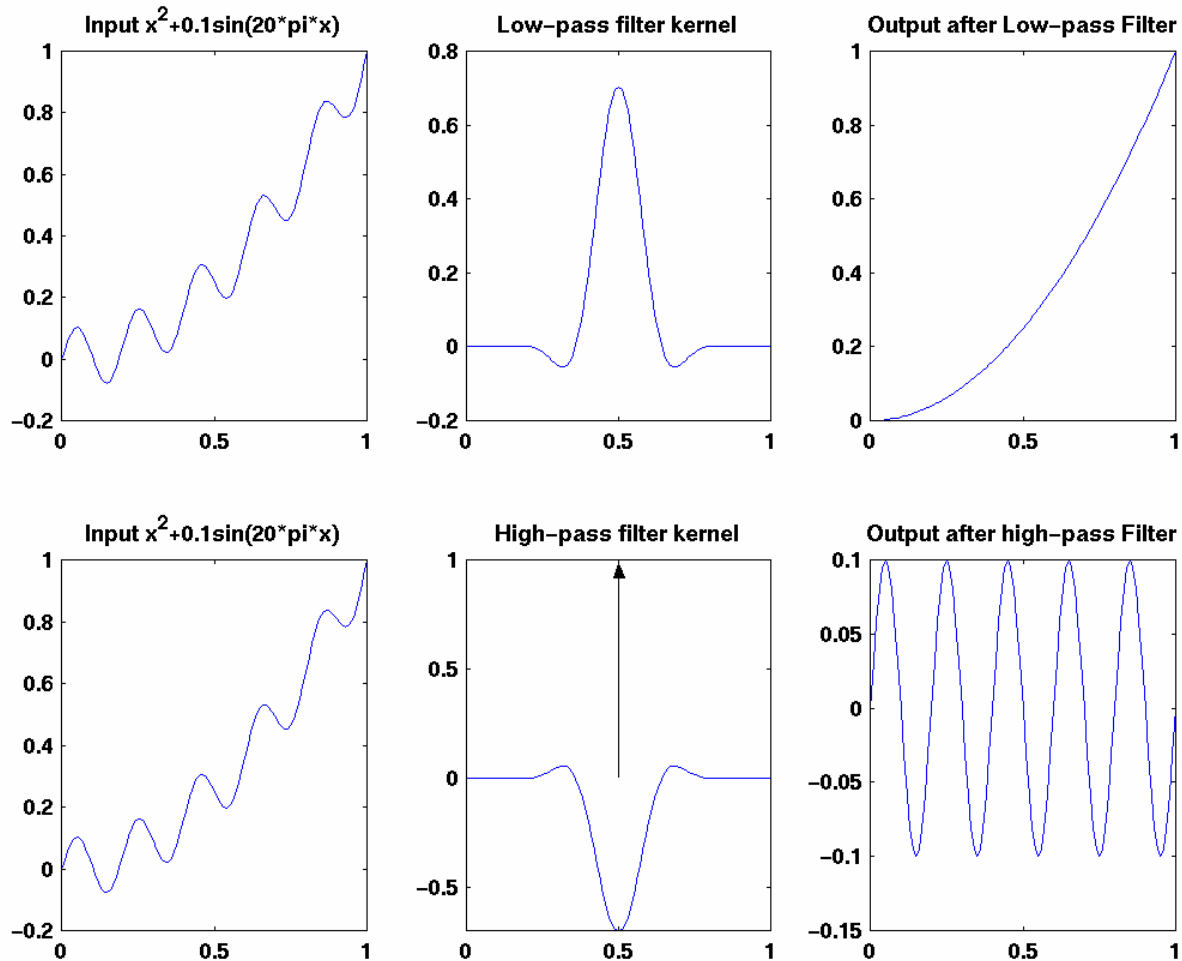
Spectral Response



UCLA



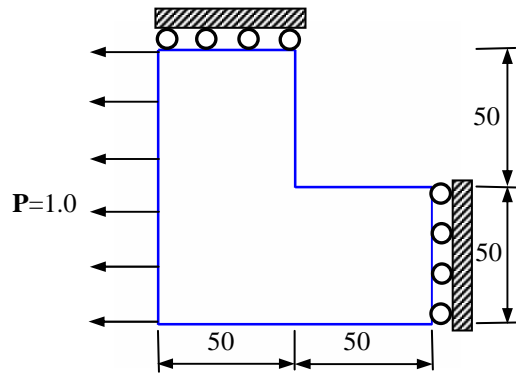
Filtering by a Reproducing Kernel



UCLA

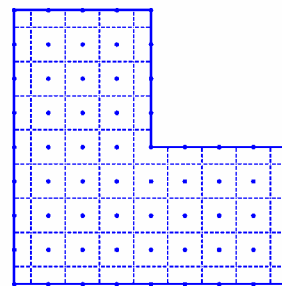


Adaptivity in L-shaped Structure

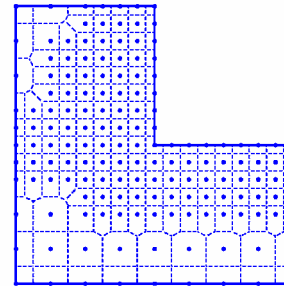


Adaptive refinement models

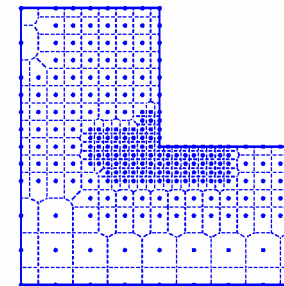
Uniformly refined model



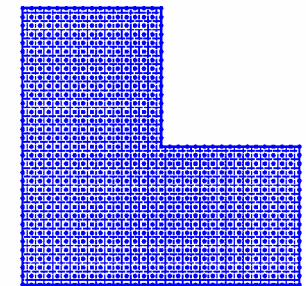
65 nodes



157 nodes

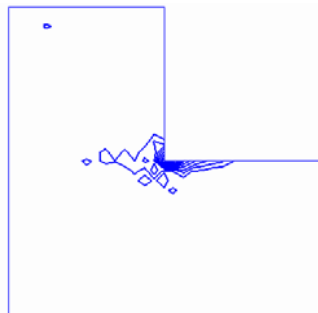


235 nodes

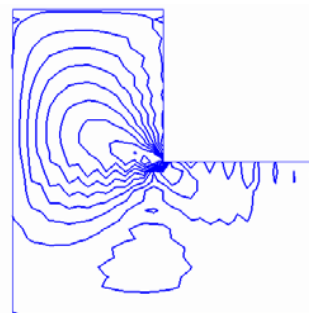


833 nodes

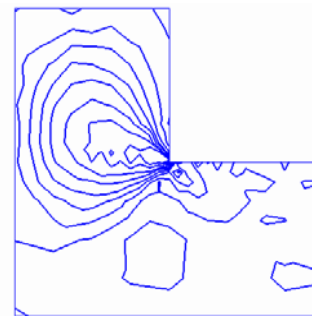
L-shaped domain in plane stress condition



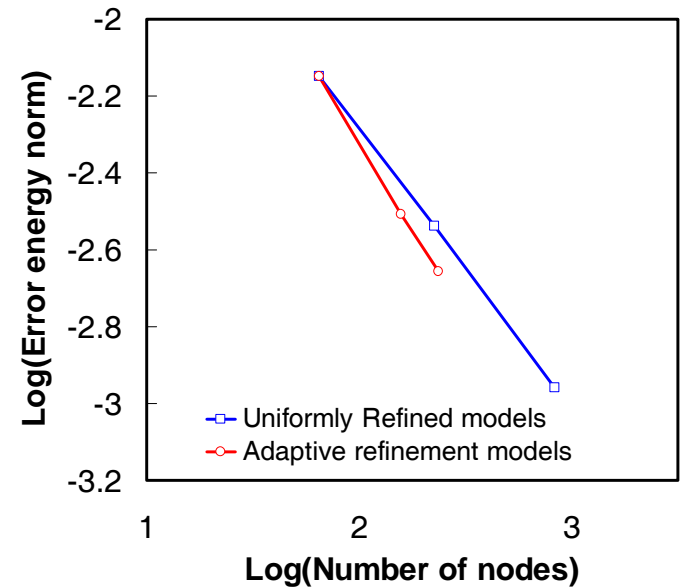
Error indicator for adaptive procedure



Stress in uniformly refined model



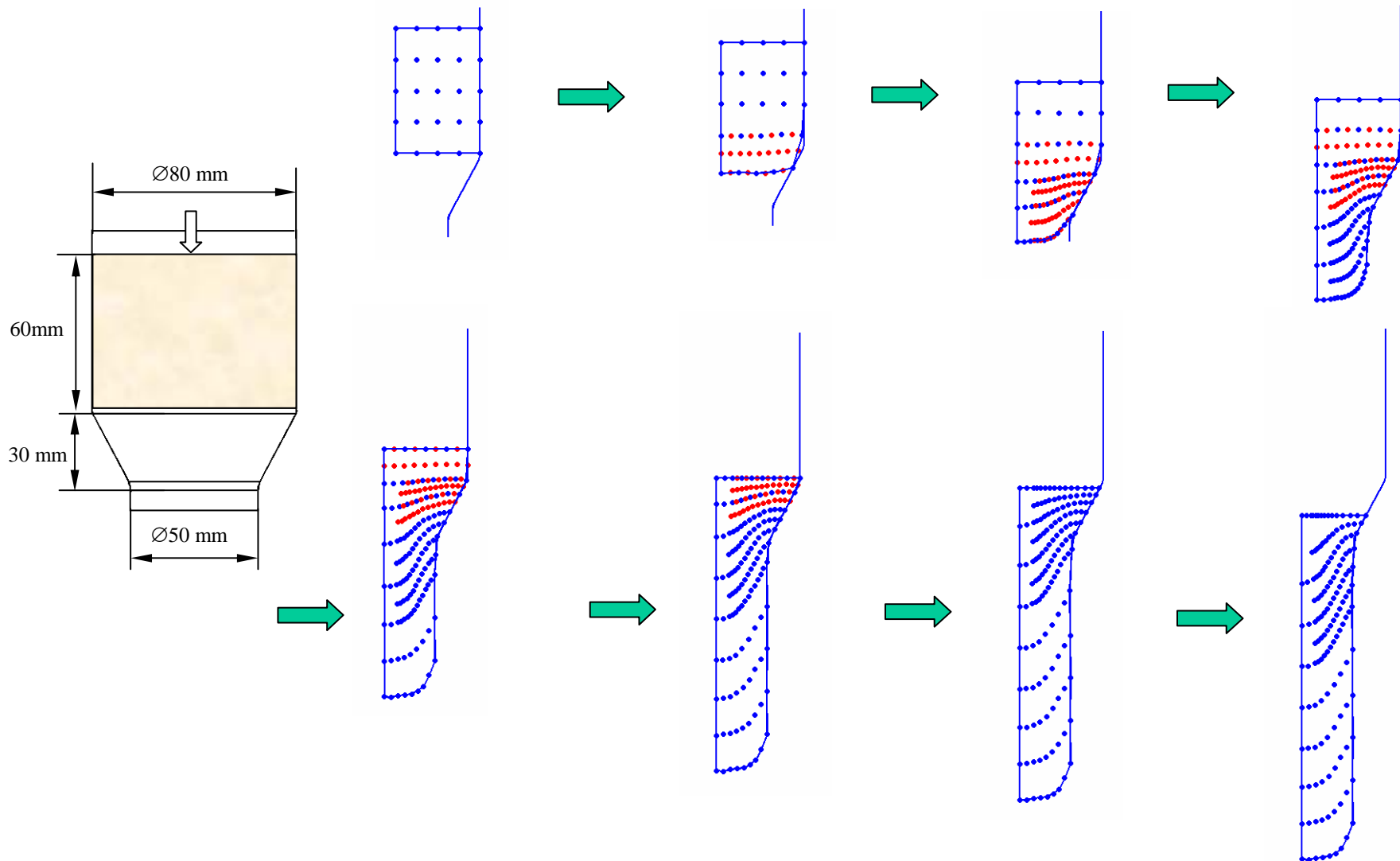
Stress in adaptive refinement model



UCLA



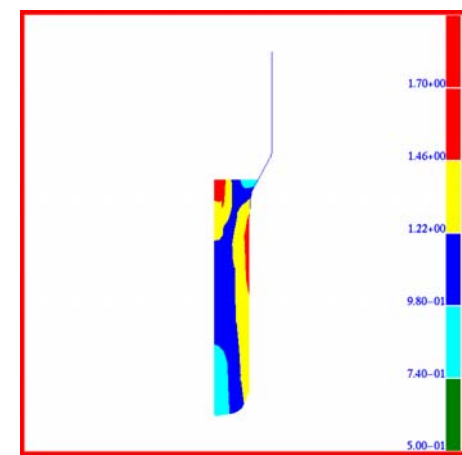
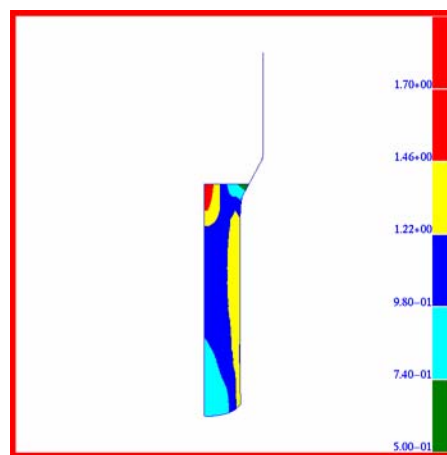
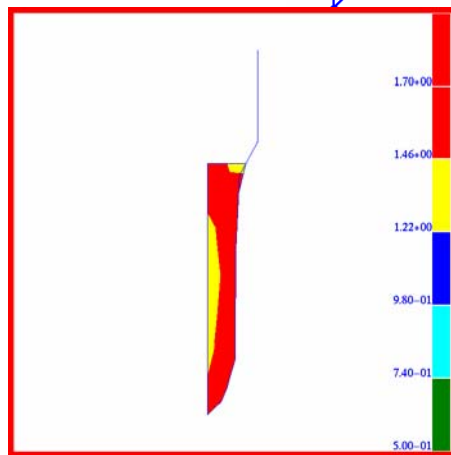
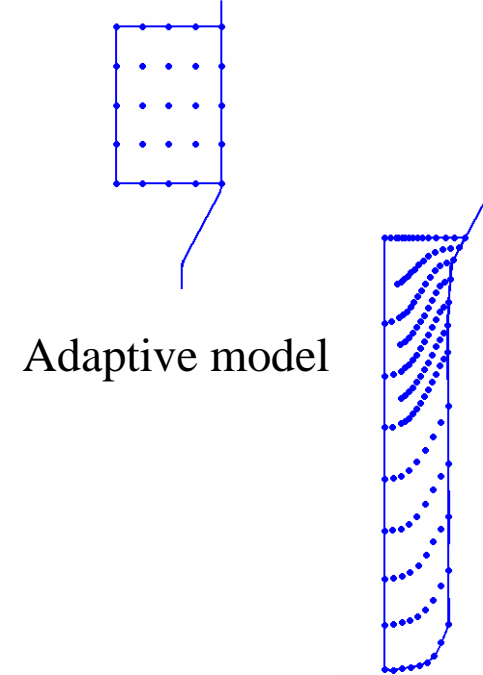
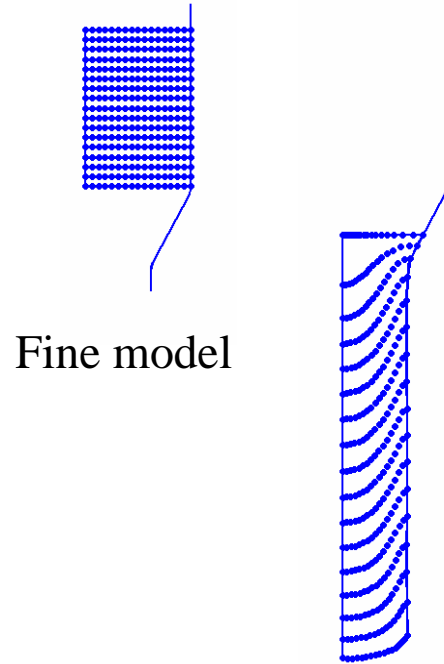
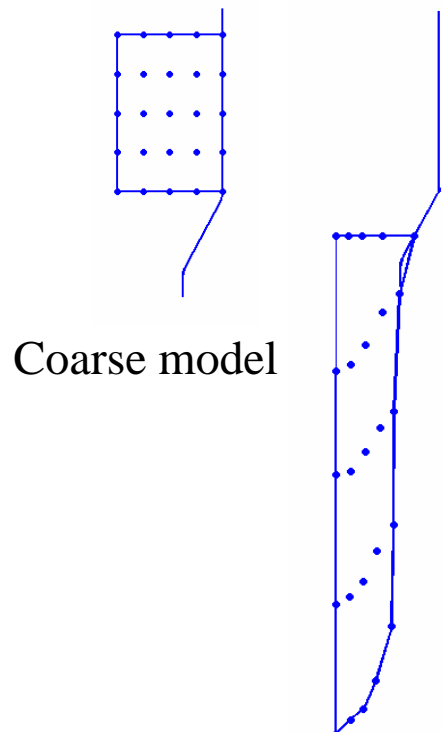
Adaptive Refinement in Metal Extrusion



UCLA



Metal Extrusion Processes



Singularity on Shell Constrained Surface

Reproducing kernel approximation is **singular** on a constrained surface S

$$\bar{\Phi}_a(\mathbf{x}; \mathbf{x} - \mathbf{x}_I) = \sum_{|\alpha| \leq 0} h_\alpha(\mathbf{x} - \mathbf{x}_I) b_\alpha(\mathbf{x}) \Phi_a(\mathbf{x} - \mathbf{x}_I)$$

where $\mathbf{x} \in S$, $\mathbf{x}_I \in S$, $S = \{\mathbf{x} : f(\mathbf{x}) = 0\}$: constrained surface

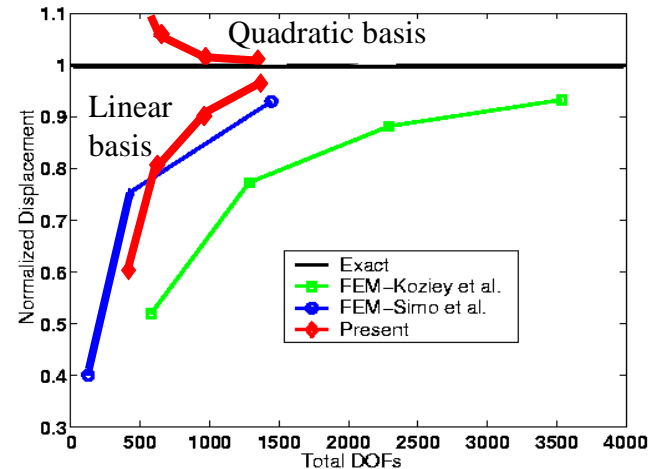
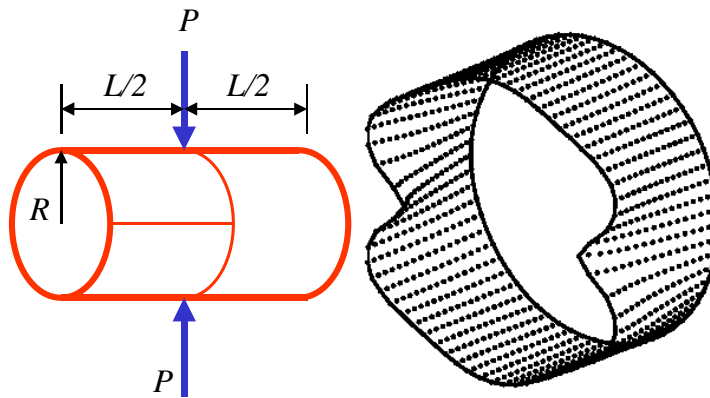
Reproducing conditions

$$\sum_I \bar{\Phi}_a(\mathbf{x}; \mathbf{x} - \mathbf{x}_I) h_{i\alpha}(\mathbf{x}_I) = h_{i\alpha}(\mathbf{x}) \quad 0 \leq |\alpha| \leq n \quad (1)$$

If $f(\mathbf{x}) = \sum_{|\alpha| \leq n} c_\alpha h_\alpha(\mathbf{x}) = 0$ Equation (1) is linearly dependent

New Approaches – Constrained reproducing kernel approximation by

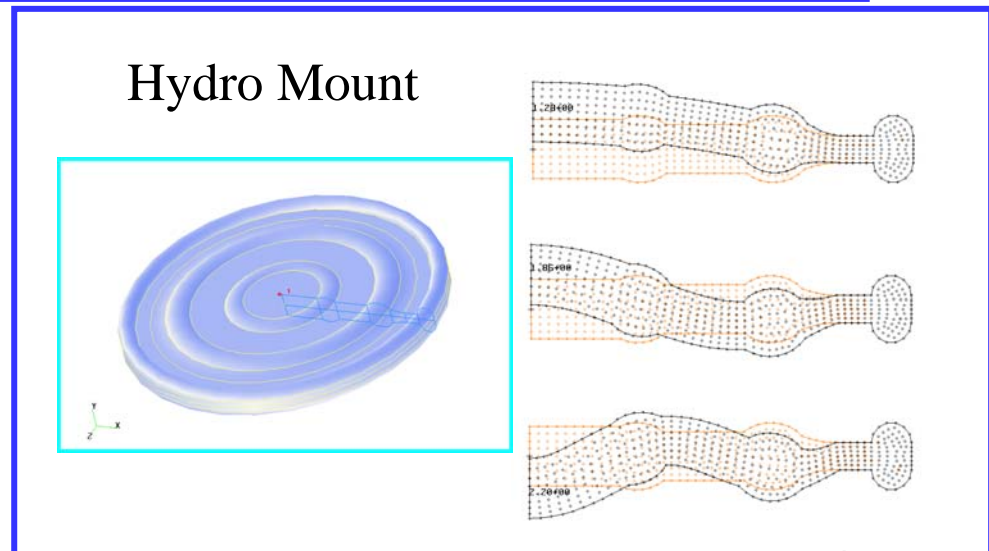
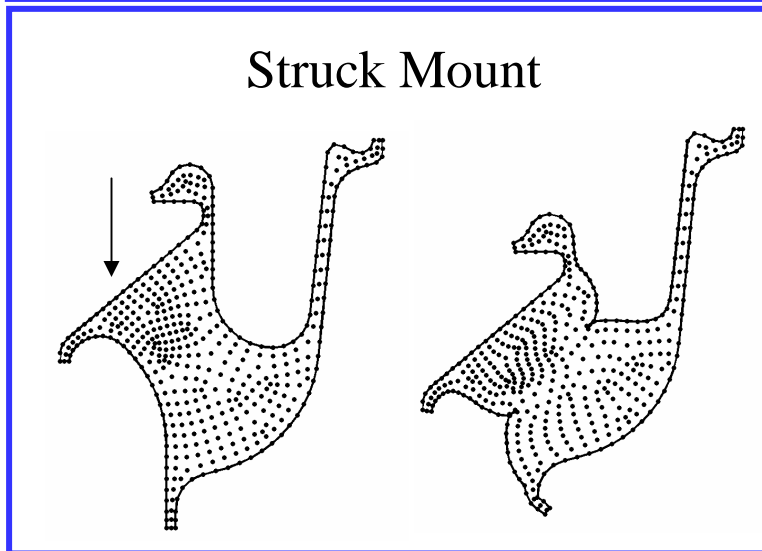
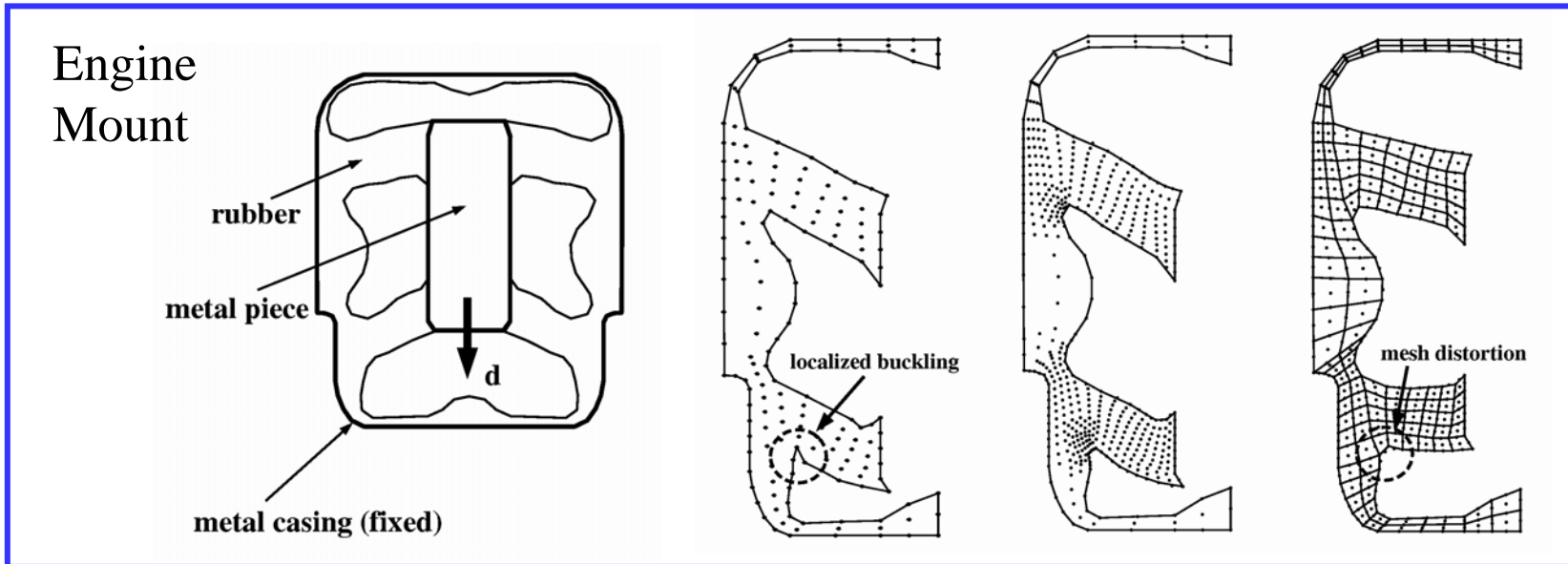
1. Dummy node method, 2. Pseudoinverse Method



UCLA

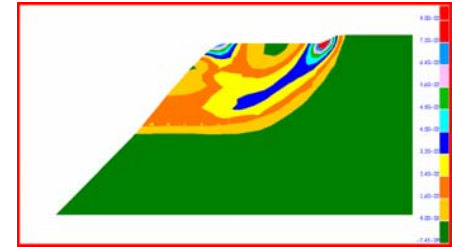
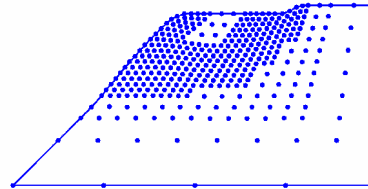
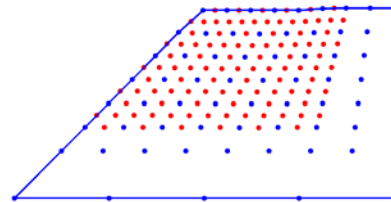
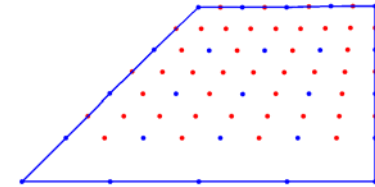
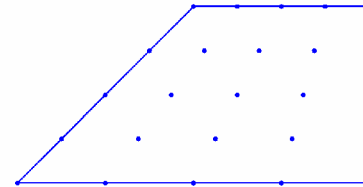
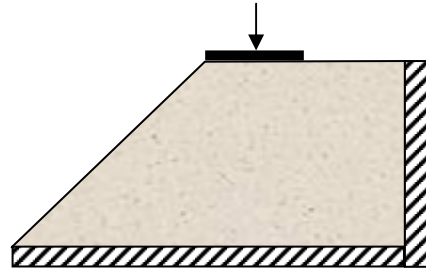


Other Applications: Elastomeric Components

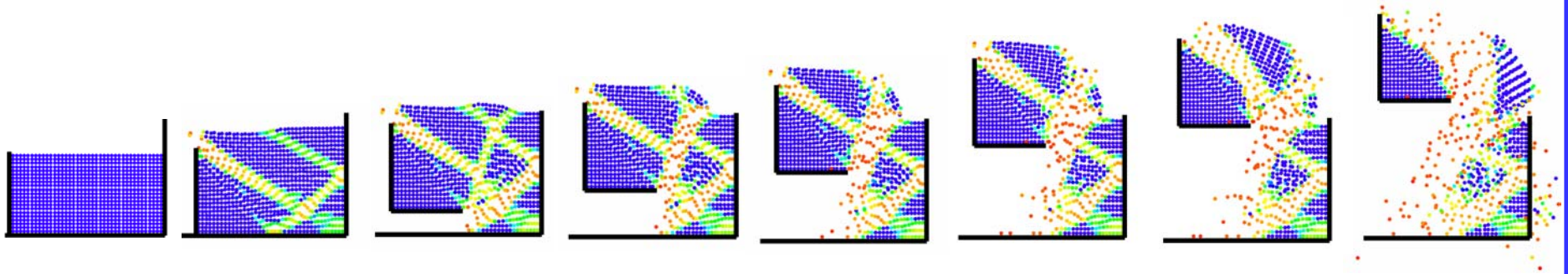


Other Applications: Geo-mechanics

Slope
Stability



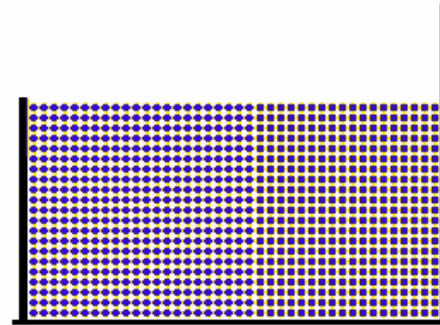
Earth Excavation



UCLA



Earth-Moving Simulation

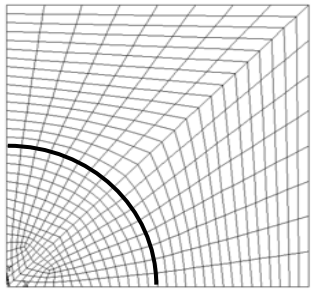


UCLA

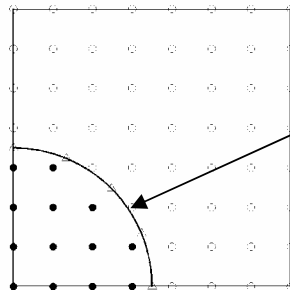


Other Applications: Magnetostrictive Particle-Filled Elastomer

FEM



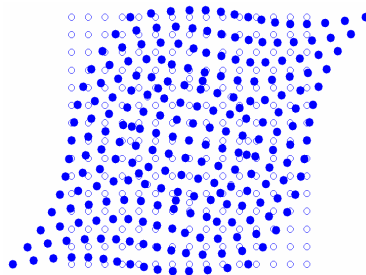
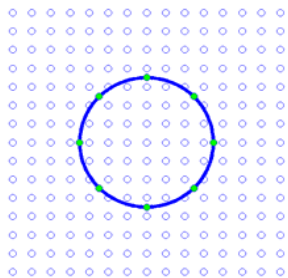
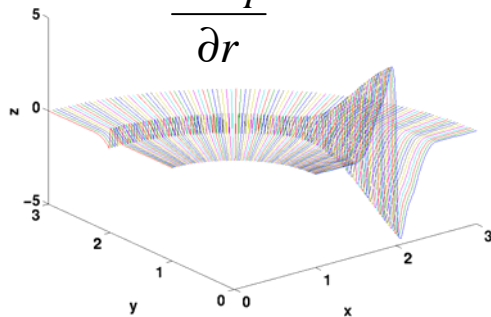
Meshfree



Interface Jump Condition

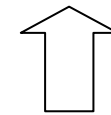
Mix Shape Function X-Derivative

$$\frac{\partial \Psi_I}{\partial r}$$

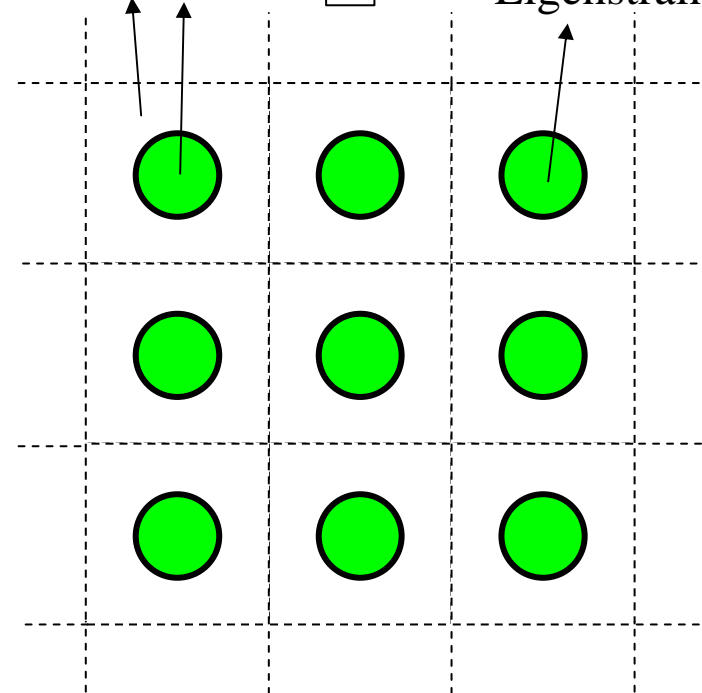


Macroscopic Field

Local Deformation



Magnetostrictive Eigenstrain

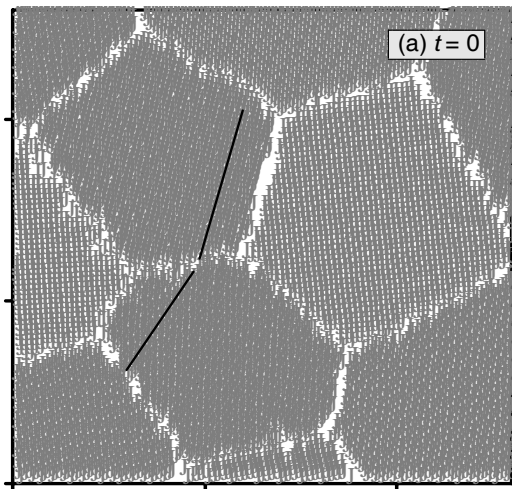


UCLA



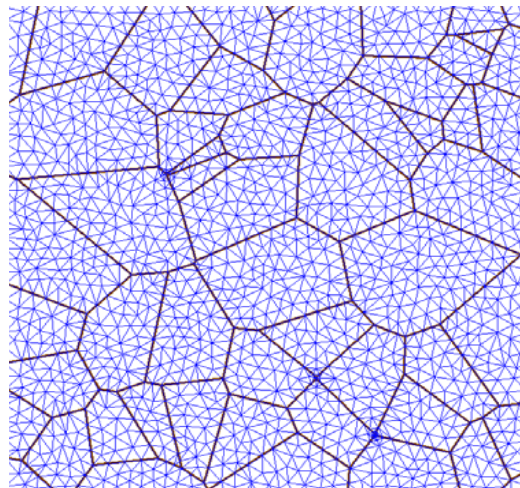
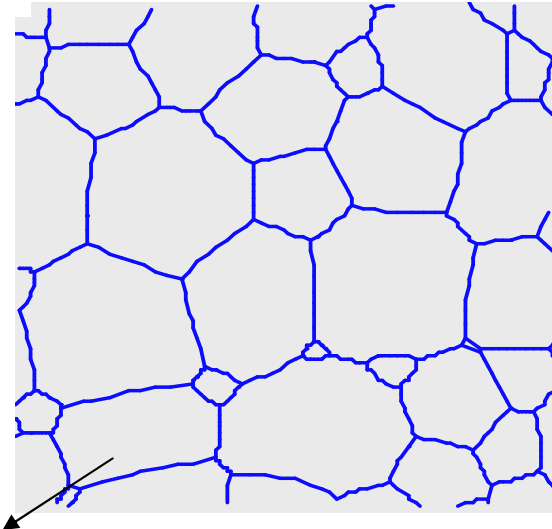
Other Applications: Microstructure Evolution

Atomistic MD simulations provide: GB properties (GB energy and mobility etc.)



Mesoscopic simulations:

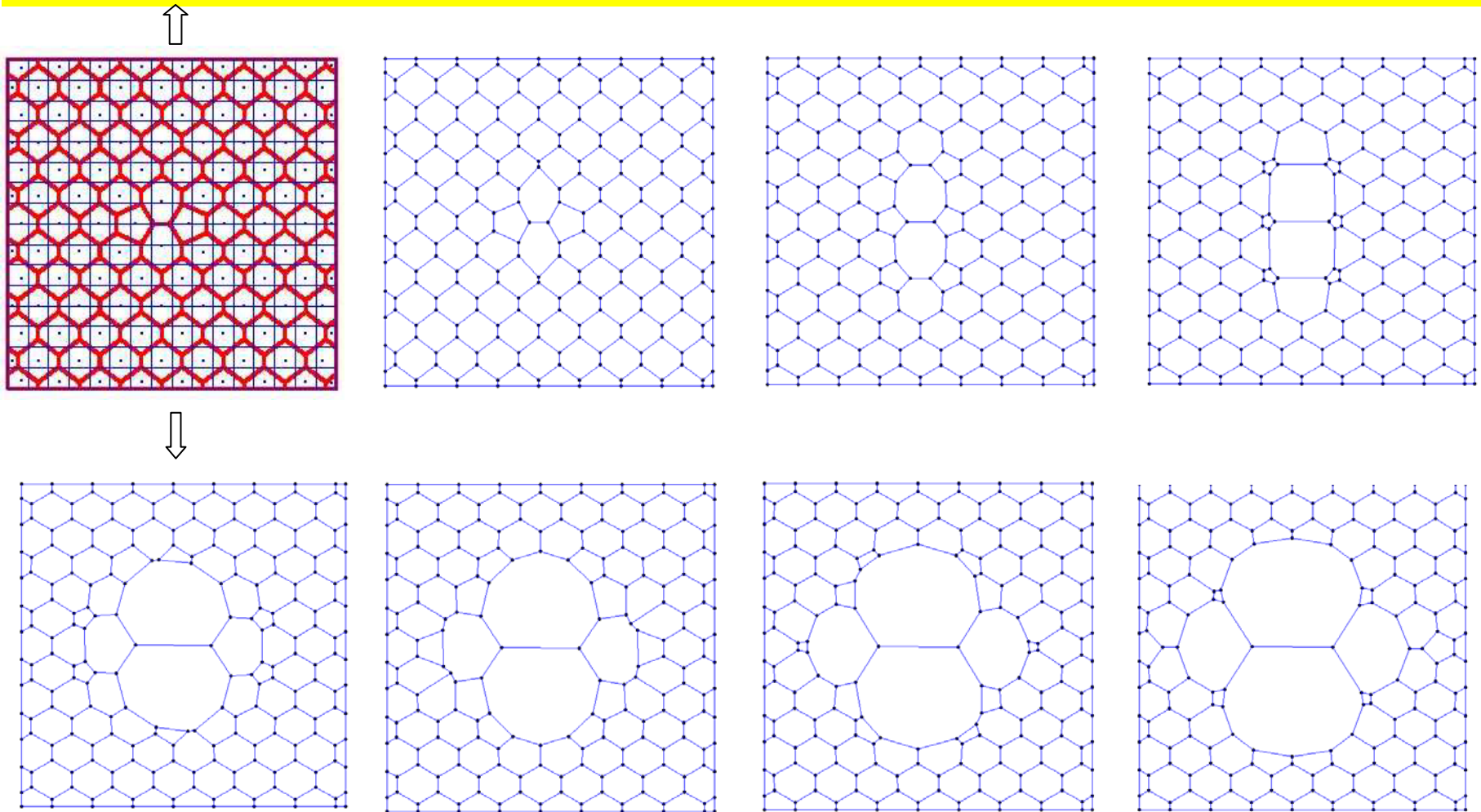
- use input GB properties from atomistic simulations
- provide statistics on systems with a large number of grains.



Finite element: Capable of bringing the externally applied stress on the system into the simulation model

Other Applications:

Meshfree Simulation of Grain Boundary Migration



Future Directions

- **Problems Involve Moving Interfaces:**
 - Microstructure evolution
 - Fluid-structure interaction
 - Solidification, welding
- **Failure and Damage Processes:**
 - Highly explosive penetration
 - Under ground/water explosion
 - Earth moving processes
 - Metal cutting
- **Multiple-scale Problems:**
 - Meso/micro/macro-scale bridging in computational material science
 - Nano systems, MEMS

